Graft Polycondensation of Microfibrillated Jute Cellulose with Oligo(L-lactic acid) and Its Properties

G. M. Arifuzzaman Khan,[1] M. Ahsanul Haque,[1] Minoru Terano,[2] Md. Shamsul Alam[1]

[1]Polymer Research Laboratory, Department of Applied Chemistry and Chemical Technology, Islamic University, Kushtia 7003, Bangladesh
[2]School of Materials Science, Japan Advanced Institute of Science and Technology, Japan
Correspondence to: M. S. Alam (E-mail: dr.alamiu@yahoo.com)

ABSTRACT: In order to improve the compatibility with different polymer matrices, microfibrillated jute cellulose (MFJC) was surface grafted by oligo(L-lactic acid) (OLA) via graft polycondensation reaction catalyzed by $Sn(Oct)_2$ in toluene medium. The effects of the OLA concentration, $Sn(Oct)_2$ concentration, reaction time, temperature, and pressure on the progress of the graft polycondensation were investigated. Maximum grafting was found 44% at optimum reaction condition. The observation was confirmed by Fourier transform infrared spectroscopy, ^{13}C-NMR spectrometry, and X-ray photoelectron spectroscopy. The morphology and crystalline structure of the graft copolymer (MFJC-g-OLA) were examined by scanning electron microscopy and wide angle X-ray diffraction, respectively. Measurements showed that initial morphological integrity of MFJC changed due to incorporation of amorphous OLA onto MFJC surface, as a result decreases crystallinity. Extracted MFJC-g-OLA was also characterized by thermo-gravimetric analysis. Results reflect the enhanced hydrophobicity and thermal stability of the MFJC as a consequence of this modification. © 2013 Wiley Periodicals, Inc. J. Appl. Polym. Sci. **2014**, *131*, 40139.

INTRODUCTION

Cellulose is the most abundant renewable biomass in the world which has a lot of advantages such as low density, low cost, good specific mechanical properties, reduced tool wear, biodegradability, and so on. It is constructed from superfine fibrils having diameters in the nanoscale and each such nanofibril contains ordered nanocrystallites and low ordered nanodomains. Its nanoscale dimensions and its capacity to form a strong entangled nanoporous network have encouraged the emergence of new high-value applications. In the last few years, a great deal of attention has been paid to microfibrillated cellulose (MFC) or nanofibrillated cellulose (NFC) composite material, which is considered one of the most promising areas of scientific and technological development.[1–3] MFC can be obtained from cellulose fibers such as wood, cotton, hemp, flax, wheat straw, rice straw, mulberry bark, ramie, tunicin, algae, hemp, flak, etc by different methods.[4] However, it is astonished that jute has rarely been used for making MFC or NCC though it is a renowned source of cellulose materials. Since jute contains high amount of α-cellulose (60–70%) and have high crystallinity (~70), it has a great prospect in the field of MFC research.

MFC shows two main drawbacks, which are associated with its intrinsic physical properties. The first one is the high number of hydroxyl groups, which lead to strong hydrogen interactions between two nanofibrils and to the gel-like structure once produced. The second limitation when MFC are used as reinforcing material in traditional composites are the dispersion of the hydrophilic cellulose in a hydrophobic matrix or a non-polar solvent as well as the difficulty to obtain good interfacial adhesion between the components in the final composite.[5] To improve the compatibility between the MFC and the polymer matrix, the reinforcing MFC can be modified physically or chemically. The most feasible solution to this is chemical surface modification to reduce the number of hydroxyl interactions and also to increase the compatibility with several matrices.[6] Up to now, various chemical methods including ring-opening polymerization (ROP),[7,8] atom transfer radical polymerization (ATRP),[9–11] reversible addition-fragmentation chain transfer (RAFT) polymerization,[12] click chemistry[13] etc. have been successfully utilized to realize the surface modification of cellulose fibers. By the aid of these approaches, different kinds of polymer chains have been covalently coupled on the cellulose surface; therefore, surface performance could be remarkably altered. However, these chemical processes are always achieved by multiple
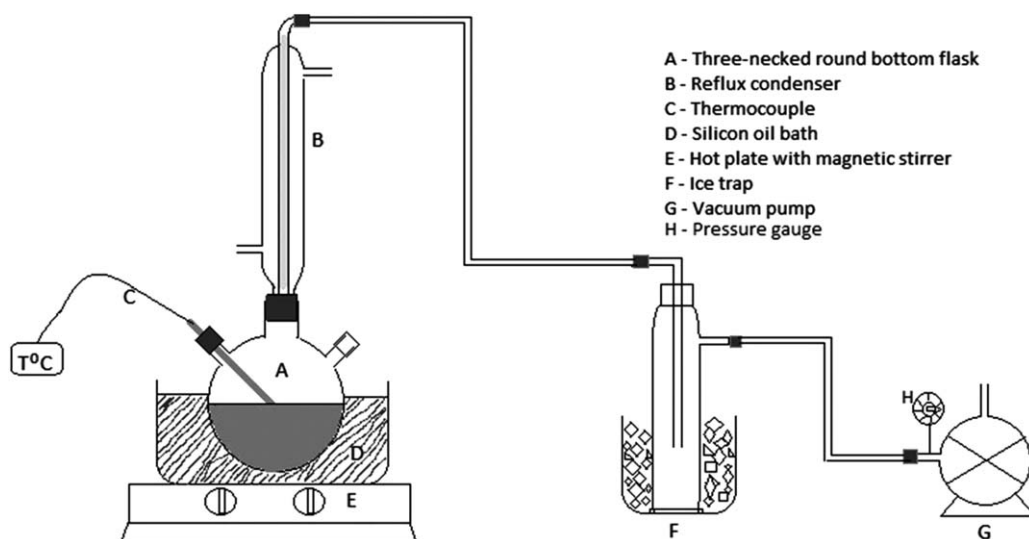
Figure 1. Graft polycondensation process of MFJC by OLA.

steps that are tedious and time consuming. Besides, a large amount of homopolymers will be formed during some grafting processes, which also makes the strategy not industrial-acceptable. One effective method for chemical modification of cellulose is to grow polymer directly off the surface, using the "grafting from" approach. By this approach, polymers have been successfully grafted from cellulose using a wide variety of polymerization techniques.[7]

Poly(L-lactic acid) (PLA), a biodegradable polymer is sometimes used for covalent modification of cellulose to increase the compatibility before fabrication of composite. Hadano et al.,[14] demonstrated the grafting of PLA to waste pulp. Further studies also showed that acetylated and deacetylated waste pulp can be grafted with PLA.[15] However, it is extremely complicated to form bond between low polar molecule like PLA (having long chain) and MFC. Relatively low molecular weight molecule such as monomer, dimmers, oligomers, etc. can be able to graft with the surface of MFC. As a consequence, several attempts are made to modify MFC by acrylic monomers.[16] However, monomer might be used in relatively large amount and needs high temperature and longer time to plasticize the MFC completely. Besides, relatively low amount of oligomers can be able to modify MFC due to their giant structure. But still now, no report has been found on the modification of MFC by oligomers.

In the present work, an effort has been made to prepare microfibrillated jute cellulose (MFJC) grafted copolymer by heterogeneous reaction of MFJC and oligo(L-lactic acid) (OLA) in toluene medium. The influencing factors on grafting were optimized. A detailed analysis of the structure of copolymer was done through spectroscopy, scanning electron microscopy (SEM), and wide angle X-ray diffraction (WAXD) measurements. The thermal properties of copolymer was analyzed and correlated with its hydrophobic nature.

EXPERIMENTAL

Materials
Jute fiber, the raw material of MFJC, was collected from local market of Jhenidha, Bangladesh and 60 cm from the middle por-

tion of the stem was taken. OLA ($M_w = 500$–900 g mol^{-1}) was synthesized from aqueous L-lactic acid (Purac, 90%) by direct polycondensation method.[17,18] Stannous octoate (Sn(oct)$_2$) and benzyl alcohol were purchased from Merck, Germany. Other chemicals used in this study were laboratory reagent grade.

Methods
About 20 g of untreated jute fiber was immersed in 1 L alkali solution (17 wt/vol % NaOH solution) for 3 h at room temperature. The alkali treated fiber was washed with distilled water and dried in air oven at 60°C for 6 h.[19] Next, 20 g of alkali treated fiber was bleached with 1 L NaClO$_2$ (7 g/L) solution buffered at pH 4 at (90–95)°C for 1.5 h maintaining the fiber-to-liquor ratio 1 : 50. After completing the bleaching reaction, the fiber was treated with 0.2 wt/vol % sodium metabisulfite solution for 15 min to reduce chlorite action, thereafter washed thoroughly with distilled water.[20] The resultant fiber contains 99–99.5 wt % α-cellulose. It was taken in $3N$ H$_2$SO$_4$ solution at room temperature maintaining the fiber-to-liquor ratio 1 : 50. The hydrolysis reaction was carried out by continuous stirring using magnetic stirrer for 3 h. MFJC was then obtained by the step filtering, washing, and drying in electric oven.

The experimental setup of graft polycondensation process of MFJC by OLA is shown in Figure 1. About 2 g of MFJC was taken in three-necked round bottom reaction flask (Pyrex). The flask was equipped with a condenser packed by 4 Å molecular sieves, vacuum pump, thermocouple, and a magnetic bar for stirring. The flask was kept in a temperature control oil bath. The OLA (50–200 wt % to MFJC), initiator-benzyl alcohol (2 wt % to MFJC), catalyst-Sn(Oct)$_2$ (0.5–2 wt % to MFJC), and 30 mL toluene were added in flask. The flask was sealed with Teflon and reaction was continued for 3, 6, and 9 h at 130–160°C under 380–76 mmHg pressure according to Table I. After completing the polycondensation, the flask was kept overnight at room temperature.

In order to remove non-grafted OLA, the MFJC-g-OLA was soaked in chloroform and stirred for 24 h. Then, the soluble OLA was filtered off, and grafted fibers were refluxed 10 times

Table I. Grafting Percentage and Moisture Content of Graft Copolymers Obtained at Various Reaction Condition

Samples	OLA conc. (wt/wt %)	Catalyst conc. (wt/wt %)	Time (h)	Temp. (°C)	Pressure (mmHg)	Grafting (%)	Grafting efficiency (%)	Moisture content (%)
MFJC-g-OLA 1	**50**	1	6	140	380	13	26	7.08
MFJC-g-OLA 2	**100**	1	6	140	380	24	24	5.84
MFJC-g-OLA 3	**200**	1	6	140	380	28	14	4.92
MFJC-g-OLA 4	100	**0.5**	6	140	380	15	15	6.99
MFJC-g-OLA 5	100	**2**	6	140	380	30	30	4.78
MFJC-g-OLA 6	100	2	**3**	140	380	12	12	7.05
MFJC-g-OLA 7	100	2	**9**	140	380	32	32	4.33
MFJC-g-OLA 8	100	2	9	**130**	380	30	30	4.76
MFJC-g-OLA 9	100	2	9	**150**	380	35	35	4.10
MFJC-g-OLA 10	100	2	9	**160**	380	27	27	5.00
MFJC-g-OLA 11	100	2	9	150	**190**	39	39	3.76
MFJC-g-OLA 12	100	2	9	150	**76**	**44**	**44**	3.14

with chloroform and 3 times with acetone. The MFJC-g-OLA was dried in vacuum oven at 60°C for 4 h and subjected for characterization. The percentage of grafting was calculated by the following formula:

$$\text{Percentage of grafting} = \frac{A-B}{B} \times 100$$

$$\text{Percentage of grafting efficiency} = \frac{A-B}{C} \times 100$$

where, A, the weight of the MFJC-g-OLA; B, the weight of MFJC; C, the weight of total OLA used.

Measurements

The Fourier transform infrared spectroscopy (FTIR) spectra of the samples were taken on Perkin–Elmer spectrometer. Samples were taken in KBr to make a transparent pellet. For each sample five scans were taken at a resolution of 4 cm^{-1}. Solid-state ^{13}C-NMR spectroscopy was measured at 25°C on a Bruker DRX NMR spectrometer at 200 MHz. X-ray photoelectron spectroscopy (XPS) was performed on a PHI 5082 spectrometer using Al Kα X-ray source operation at 15 kV under a current of 24 mA. Samples were placed in an ultra high vacuum chamber with photoelectron collector by a hemispherical analyzer at taken off angle of 45°. Moisture contents in MFJC-g-OLA were measured by an electric oven.

WAXD patterns were obtained with a BRUKER D8 ADVANCE wide angle X-ray diffractometer using Cu Kα radiation ($\alpha = 0.154$ nm), voltage of 50 kV, and current of 40 mA with 2θ ranges from 5° to 45° increase in steps of 2°/min.

The surface morphology of MFJC samples were observed by scanning electron microscope (FEI QUANTA 200 3D) with an accelerating voltage 10 kV. The surface was coated with 3 nm thick gold before analysis.

The thermogravimetry of MFJC samples were conducted by thermal gravimetric analyzer (TG/DTA 6300, Seiko Instrument, Japan). About 20 mg of each sample was taken for analysis. The samples were heated up steadily at a rate of 20°C/min from 25 to

600°C under continuous flow of nitrogen at 50 mL/min. To get perfection, analysis was carried out two times for each sample.

RESULTS AND DISCUSSION

Effect of Reaction Parameters on Graft Polycondensation

Graft polycondensation was conducted under different reaction condition in toluene as a reaction medium. Polycondensation byproduct water is efficiently removed by using the high boiling-point solvent.[21] However, the system was heterogeneous throughout the polycondensation, due to insolubility of MFJC in toluene which is a good solvent of OLA. During graft polycondensation reaction, OLA concentration, catalyst concentration, reaction time, temperature, and pressure were varied to optimize grafting reaction. The grafting percentage and grafting efficiency with those parameters are shown in Table I.

The effect of the OLA concentration on the grafting was studied under predetermined conditions. It influences the graft polycondensation to adjoining required number of oligomer units onto MFJC during the reaction. To analyze the effect of the monomer concentrations, the concentrations of the catalyst were kept constant at 1 wt/wt % with respect to the weight of MFJC. The reaction was carried out at 140°C for 6 h. OLA was taken in reaction flask with 50, 100, and 150 wt/wt % with respect to the weight of MFJC. The result shows that there was very less polycondensation reaction occurring at low OLA concentrations. However, the percentage of grafting increases with the increase of OLA concentration whereas grafting efficiency decreases. With the increase of OLA concentration, the numbers of OLA molecule increase which are attached to form graft polymer hence increase grafting. In low concentration, relatively greater number of OLA is activated by the action of initiator and catalyst.[8,22] Therefore, 50 wt/wt % OLA shows highest grafting efficiency.

The effect of the catalyst concentration on the grafting yield was studied through the variation of the Sn(Oct)$_2$ concentration from 0.5 to 2 wt/wt %. It is also found that grafting percentage and grafting efficiency increases with increase of catalyst
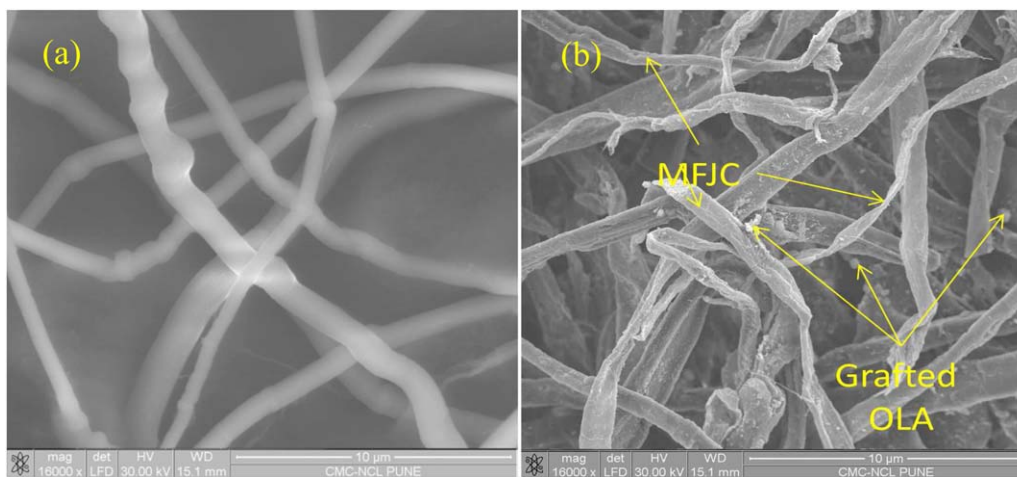
Figure 2. SEM photograph of (a) MFJC and (b) MFJC-*g*-OLA 12. [Color figure can be viewed in the online issue, which is available at wileyonlinelibrary.com.]

concentration. Catalyst $Sn(Oct)_2$ activated cyclic OLA or lactide molecule in the presence of benzyl alcohol initiator for grafting reaction.[22] Hence, higher concentration of catalyst produced more activated OLA which enhanced grafting.

Table I shows the changes in grafting percentage as a function of reaction time at 140°C and 760 mmHg pressure during the graft polycondensation processes. According to result, the early stage of the polycondensation, both the grafting percentage and efficiency were low. The percentage of grafting increased rapidly after 6 h and highest amount of grafting occurred at 9 h of grafting and efficiency percentages both of 32%. It implies that equilibrium of this graft polycondensation reaction might have taken longer time.

The changes of grafting percentage as a function of reaction temperature during the graft polycondensation are shown in Table I. It is evident that high temperature promotes the water removal through esterification reaction; therefore polycondensation of OLA and grafted MFJC as well as non-grafted hydroxyl group may be increased. Besides, the catalyst $Sn(Oct)_2$ might be more activated at higher temperature and thus the propagation

rates of grafting were accelerated. Both the percentage of grafting and the efficiency increased to 35% at the reaction temperature up to 150°C. However, the grafting percentage and efficiency both were declined when the temperature was elevated beyond 150°C, possibly due to hydrolytic action, thermal degradation, and intramolecular esterification of OLA.
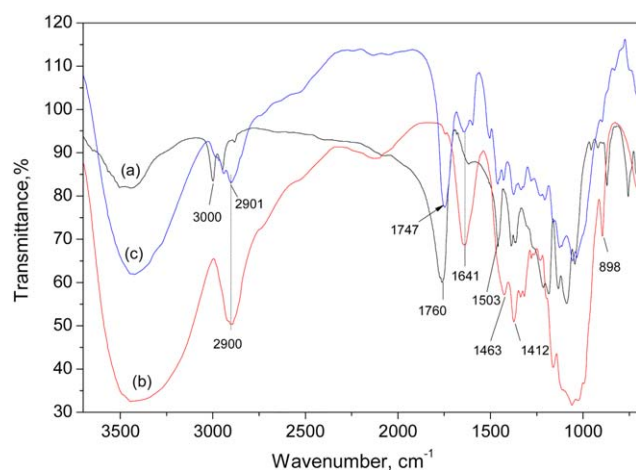

Figure 3. FTIR spectra of (a) OLA, (b) MFJC, and (c) MFJC-*g*-OLA 12. [Color figure can be viewed in the online issue, which is available at wileyonlinelibrary.com.]
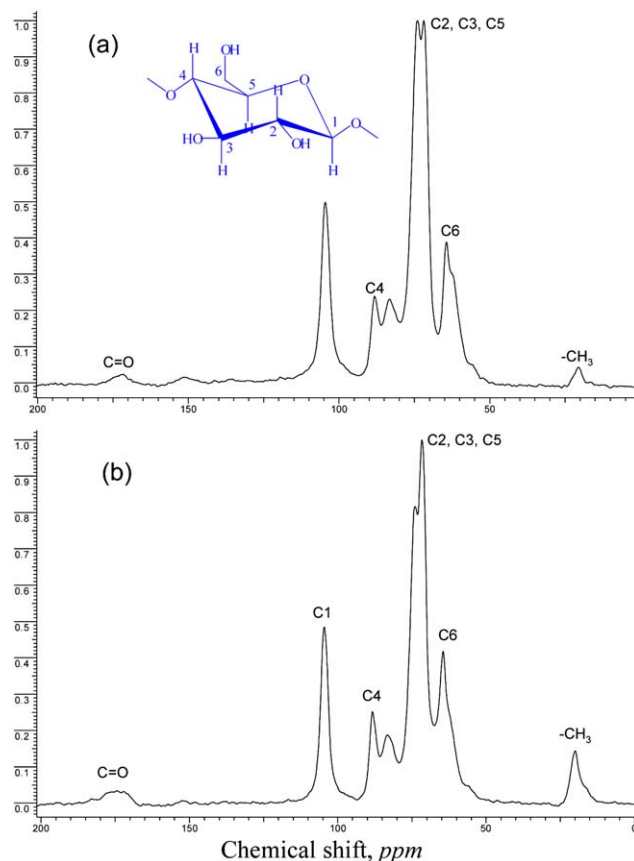

Figure 4. ^{13}C-NMR spectra of (a) MFJC and (b) MFJC-*g*-OLA 12. [Color figure can be viewed in the online issue, which is available at wileyonlinelibrary.com.]
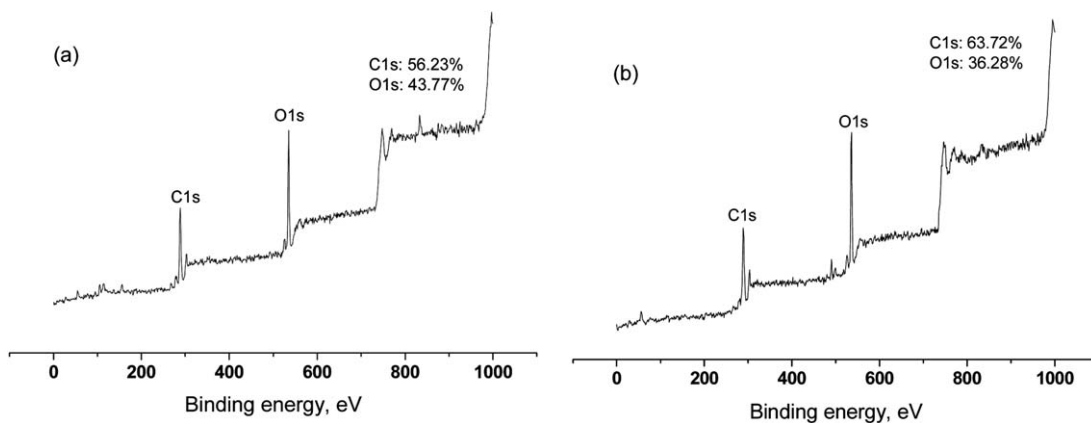
Figure 5. Overall XPS spectra of (a) MFJC and (b) MFJC-*g*-OLA 12.

The effect of pressure on the percentage of grafting was studied through the variation of pressure from 380 to 76 mmHg. The percentage of grafting and grafting efficiency both were increased to 44%, when the pressure was 76 mmHg. As predicted, the graft polycondensation reaction proceeded much faster to forward direction when the water was continuously eliminated by reduction of pressure.[23,24] For this reason, the chain lengths of grafted OLA may increase at much higher rate and hence increase grafting.

Moisture Content of MFJC-g-OLA

Moisture content of the MFJC-*g*-OLA samples were measured at 50% relative humidity at 30°C for 24 h and then dried in oven at 60°C for 30 min. Moisture content % is calculated as follows:

$$\text{Moisture content \%} = \frac{W_i - W_f}{W_i} \times 100$$

where, W_i, the weight before drying; and W_f, the weight after drying.

The effect of graft yield on the moisture content is shown in Table I. It can be seen that with increasing of grafting percentages, the moisture content reduces. This may be because OLA form hydrophobic polymer during graft polycondensation reaction onto cellulose chain and filling of pith channel caused reduction of moisture content. With the increasing of OLA on the MFJC may fill up the capillary spaces present on the surface and inside the fibrills and cover up the fibrill surfaces with the hydrophobic materials. Scanning electron micrograph of MFJC-*g*-OLA 12 also clearly shows that OLA molecules are grafted or coated on MFJC surface (Figure 2). Since MFJC-*g*-OLA 12 shows more hydrophobic nature, it will more compatible with hydrophobic polymer matrices.

Spectroscopic Analysis

Before characterization by FTIR, ^{13}C-NMR, and XPS spectroscopy, the MFJC-*g*-OLA 12 was washed according to the mentioned procedure. Figure 3 shows the FTIR spectra of OLA, MFJC, and MFJC-*g*-OLA 12. The MFJC spectrum shows distinctive peaks and bands for carbohydrates: a broad band in the range of 3760–3010 cm^{-1} indicates hydrogen bonded hydroxyl groups, CH$_2$
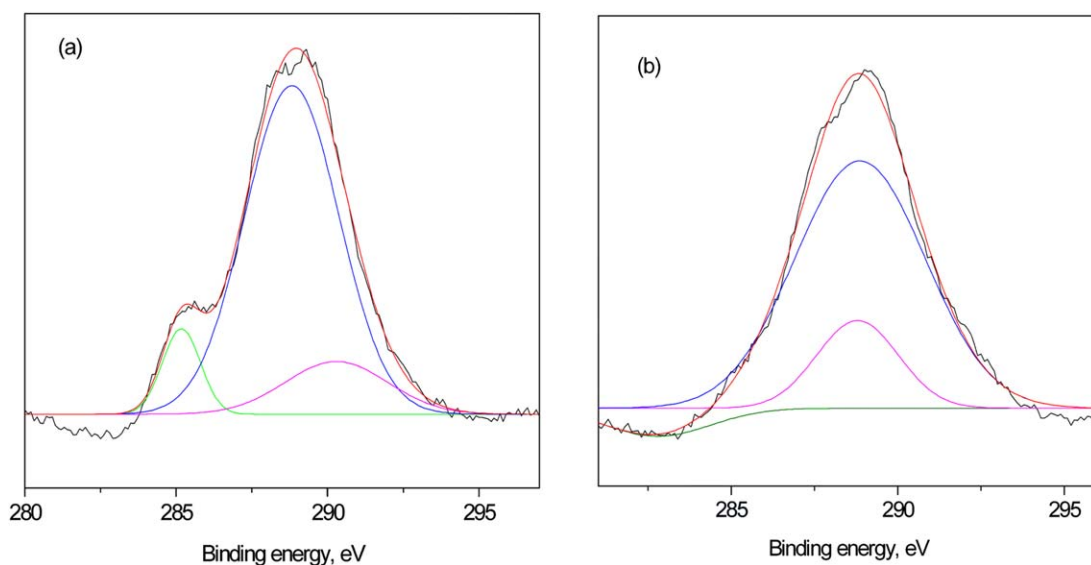

Figure 6. C1s XPS spectra of (a) MFJC and (b) MFJC-*g*-OLA 12. [Color figure can be viewed in the online issue, which is available at wileyonlinelibrary.com.]

Figure 7. O1s XPS spectra of (a) MFJC and (b) MFJC-*g*-OLA 12. [Color figure can be viewed in the online issue, which is available at wileyonlinelibrary.com.]
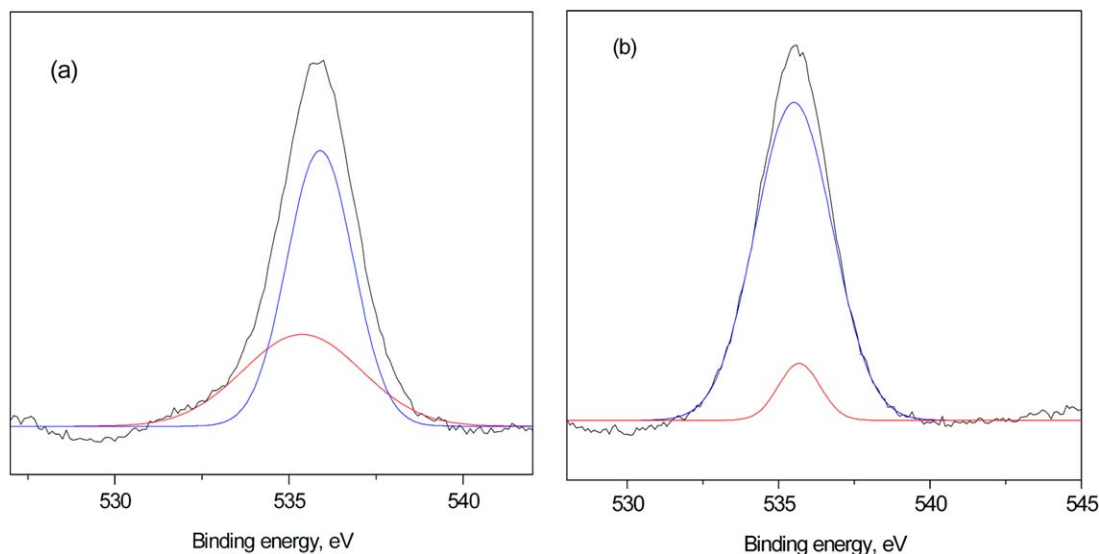
Table II. C1s XPS Spectra of MFJC and MFJC-*g*-OLA 12

| Band no.	Peak position		Location of carbon atom	Total area (%)	
	MFJC	MFJC-*g*-OLA 12		MFJC	MFJC-*g*-OLA 12
1	285.17	–	—C*—O—C—	8.23	–
2	288.81	288.79	—C*—OH/O—C*—O	78.13	16.86
3	290.28	289.87	O—C*=O	13.64	76.14

stretching at 2932 cm^{-1}, O—C stretching in the range of 1180–960 cm^{-1}, and anhydroglucose ring stretching vibrations in the range 861–575 cm^{-1}.[25] On the other hand, FTIR spectra of OLA shows a well-defined absorption at 1762 cm^{-1} owing to the ester carbonyl, peaks at 1200–1000 cm^{-1} to the C—O stretch, and peaks at 2850–2960 cm^{-1} to the stretch of CH and CH$_3$ groups respectively. Besides, the FTIR curve of MFJC-*g*-OLA 12 bears dual characteristics of OLA and MFJC. Due to the absence of carbonyl group, MFJC does not show any peak at around 1700–1760 cm^{-1}. MFJC-*g*-OLA 12 demonstrates an additional intense peak at about 1747 cm^{-1} region, which is arising from the stretching of carbonyl group of ester. In addition, the relative intensity of the characteristic peak of MFJC decreases at around 3400 cm^{-1}for MFJC-*g*-OLA 12 which is responsible for hydrophilic —OH band stretching in MFJC. Characteristics peak of CH$_2$ group of the

OLA at 3000 cm^{-1} is absent in case of MFJC-*g*-OLA 12 probably due to bond formation.

Solid-state ^{13}C-NMR spectroscopy was used to characterize the synthesized MFJC-*g*-OLA. The typical ^{13}C-NMR spectra in Figure 4(a,b) show the peaks in the range of 50–120 ppm for C1–C6 carbon of cellulose anhydroglucose unit. Two very small signals at 175 and 19 ppm appears due to the carbonyl group (C=O) and methyl group (—CH$_3$), respectively, of MFJC.[26] However, ^{13}C-NMR spectrum of MFJC-*g*-OLA 12 illustrates relatively intense peaks at the same position (175 and 19 ppm). The increase in the intensity of C=O and —CH$_3$ peaks in the spectrum of MFJC-*g*-OLA 12 indicates the presence of carboxyl groups and methyl groups of OLA. In addition, the carbonyl (C=O) group might have appeared from the esterification reaction of hydroxyl groups of MFJC and carboxyl group of OLA.

Table III. O1s XPS Spectra of MFJC and MFJC-*g*-OLA 12

Band no.	Peak Position		Location of carbon atom	Total area (%)	
	MFJC	MFJC-*g*-OLA 12		MFJC	MFJC-*g*-OLA 12
1	535.38	535.49	—C—O*—C—/-C=O*	37.35	91.22
2	535.90	535.90	—C—O*H	62.65	8.78
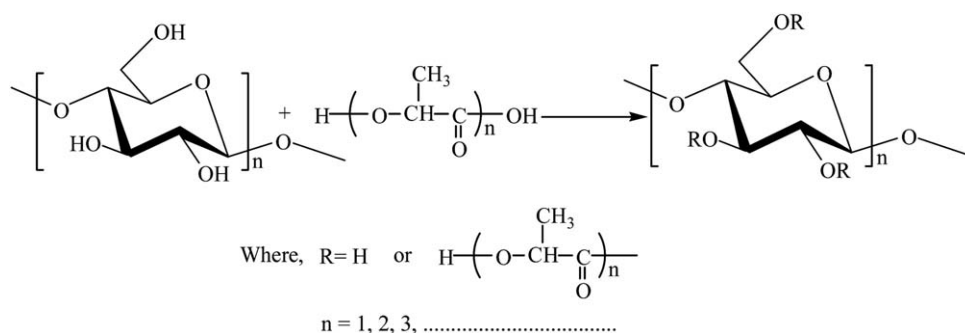
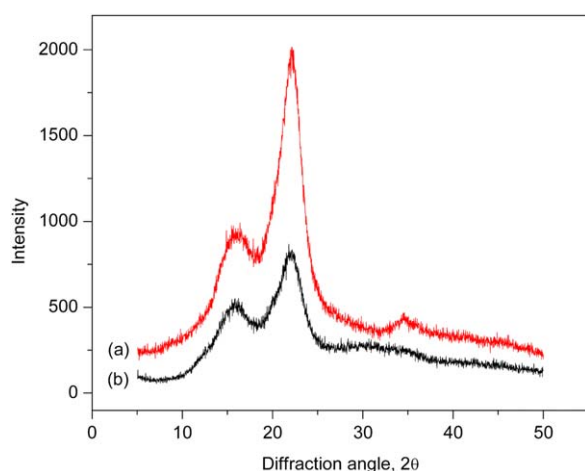**Scheme 1.** Possible interaction mechanism between MFJC and OLA.

Figure 8. WAXD spectra of (a) MFJC and (b) MFJC-*g*-OLA 12. [Color figure can be viewed in the online issue, which is available at wileyonlinelibrary.com.]

Thus the result shows the presence of OLA functional groups in MFJC and is in agreement with a previous report.[27]

XPS provides a suitable tool to analyze the variation in chemical composition of the MFJC surface due to the graft polycondensation (Figures 5–7). Carbon and oxygen atoms are the main constituents of MFJC before and after grafting, and the corresponding atomic content can be quantitatively determined from the integration of C1s and O1s signals. After the grafting process, the C/O ratio has been evidently increased because the MFJC-*g*-OLA 12 has a higher carbon atomic fraction.[28]

More detailed analysis has been performed through the deconvolution of the high-resolution C1s and O1s signals (Figures 6 and 7). The decomposed multiple peaks have been assigned to the corresponding functional groups with the correlative data summarized in Tables II and III, respectively. Results demon-strate that C1s spectrum of MFJC-*g*-OLA 12 exhibits the absence of signal at 285.17 eV (—C*—O—C—) and the area increases significantly for —C*=O at 289.87 eV may be due to esterification reaction. Moreover, O1s signals of MFJC-*g*-OLA 12 shows greater area of the peak at 535.49 eV which is respon-sible for —C=O*/—C—O*—C— bond and lowering the area of the peak at 535.90 eV which is responsible for —C—O*H bond (Figure 7). Therefore, XPS data proved that esterification link-age is present in between MFJC and OLA. The possible reaction between the hydroxyl (—OH) groups in cellulose and OLA is illustrated in Scheme 1. The linking of MFJC and OLA was by the formation of a chain of covalent chemical bonds.

WAXD Analysis

The crystalline structure of MFJC and MFJC-*g*-OLA 12 was examined by WAXD measurements. Figure 8 illustrates WAXD intensity profiles obtained for powder samples of MFJC and MFJC-*g*-OLA 12. MFJC shows the strongest diffraction peak at $2\theta = 15.6°$, $22.5°$, and $34.5°$. The major crystalline peaks posi-tioned at around $2\theta = 15.6°$ and $22.5°$ represent the cellulose crystallographic $(10\bar{1})$ and (002) plane, respectively. Compared with the MFJC, there was no crystalline transformation of the crystalline structure in MFJC-*g*-OLA 12 due to invisible changes in the diffraction angle (2θ). However, the relative diffraction intensity was decreased for indicating graft copolymers synthe-sized in the present study. This suggests that the grafted OLA spreads the distance between MFJC molecules and decreases crystallinity. Similar results also found for CDA-*g*-PLLA copoly-mers in the study by Teramoto and Nishio.[29]

Thermal Properties of MFJC-g-OLA

The thermal stability of graft copolymers was also evaluated by thermo-gravimetric analysis (TGA), as shown in Table IV and Figure 9. The decomposition behavior of MFJC-*g*-OLA 12 is similar to that of neat MFJC because the primary composi-tions (i.e., glucose units) in both copolymers are the same. The

Table IV. Thermal Properties of MFJC-*g*-OLA 12

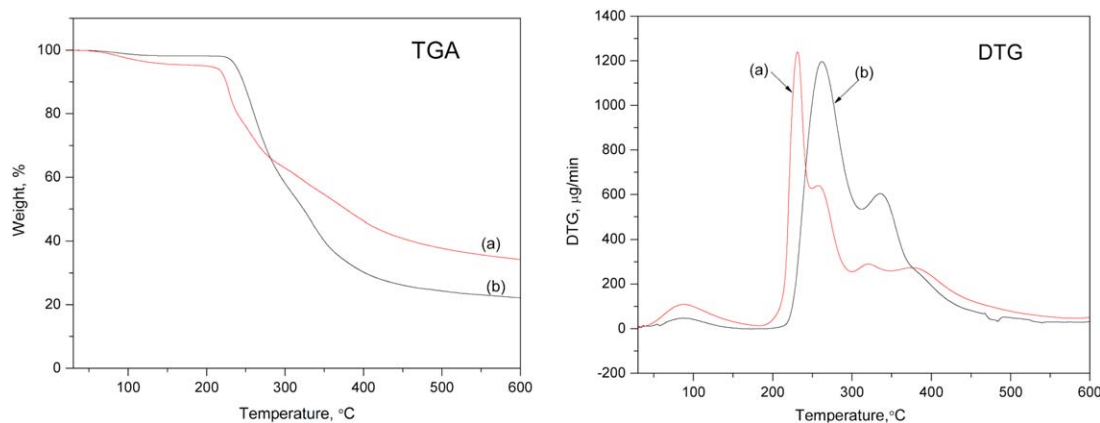| Samples	Weight loss % at the temp. range		Charge residue at 600°C (%)	DTG (µg/min)	
	30–130°C	180–450°C		Peak 1	Peak 2
MFJC	4.1	48.3	35.1	1.229 (229°C)	0.45 (250°C)
MFJC-*g*-OLA	1.5	70.7	23.1	1.190 (261°C)	0.60 (335°C)

Figure 9. TGA and DTG thermograms of (a) MFJC and (b) MFJC-*g*-OLA 12. [Color figure can be viewed in the online issue, which is available at wileyonlinelibrary.com.]

initial weight loss at 30–130°C for moisture removal is found lower in case of MFJC-*g*-OLA 12. The grafting of OLA substantially decreases the hydrophilicity of MFJC. The main degradation was started at about 190°C and completed at 450°C. The weight loss of MFJC-*g*-OLA 12 at this stage is 70.7% whereas weight loss of MFJC is 48.3%. The grafted chain of OLA may be degraded along with MFJC. Hence, weight loss is more prominent for MFJC-*g*-OLA 12. At 600°C, the residual weight of MFJC-*g*-OLA 12 is about 23 wt %, which is lower to that of MFJC under similar conditions. The main residues are attributed to the formation of char, because the decomposed products are easily volatilized and have been blown out during the heating process.[28] Figure 9 also shows the first derivative curve (DTG), as a function of temperature, obtained from the thermograms. The DTG curve of the MFJC and MFJC-*g*-OLA 12 shows the multi-stage degradation due to different number anhydroglucose unit present in microfibril. The broadened decomposition peaks of MFJC-*g*-OLA 12 reflect the improved thermal stability by grafting.

CONCLUSION

MFJC was successfully grafted with OLA in the presence of Sn(Oct)$_2$/benzyl alcohol catalyst system. Maximum percentage of grafting found (44%) at the reaction condition: 100 wt/wt % OLA concentration, 2 wt/wt % Sn(Oct)$_2$ concentration, time 9 h, temperature 150°C, and pressure 190 mmHg. Among the graft copolymers, MFJC-*g*-OLA 12 (graft yield 44%) revealed more hydrophobic nature and hence it will be more compatible with non-polar polymer matrices. The types of bonding, binding energy, and crystallinity in MFJC-*g*-OLA 12 copolymer were studied by spectroscopic analysis and WAXD measurement. Scanning electron micrograph also supported the formation of graft copolymer onto MFJC surface. As a consequence, the resultant copolymer had a high resistance toward the thermal degradation. The length of grafted chain and degree of substitution in copolymer will be studied in further study.

ACKNOWLEDGMENTS

REFERENCES

1. Dufresne, A. In Cellulose-Based Composites and Nanocomposites, In Monomers, Oligomers, Polymers and Composites from Renewable Resources; Belgacem, M. N.; Gandini, A., Eds.; Elsevier, Amsterdam, **2008**.

2. Song, Y.; Tashiro, K.; Xu, D.; Liu, J.; Bin, Y. *Polymer* **2013**, *54*, 3417.

3. Aranguren, M. I.; Marcovich, N. E.; Salgueiro, W.; Somoza, A. *Polym. Test.* **2013**, *32*, 115.

4. Klemm, D.; Kramer, F.; Moritz, S.; Lindström, T.; Ankerfors, M.; Gray, D.; Dorris, A. *Angew. Chem. Int. Edit.* **2011**, *50*, 5438.

5. Samir, M. A. S. A.; Alloin, F.; Dufresne, A. *Biomacromolecules* **2005**, *6*, 612.

6. Gousse, C.; Chanzy, H.; Excoffier, G.; Soubeyrand, L.; Fleury, E. *Polymer* **2002**, *43*, 2645.

7. Hafreèn, J.; Coòrdova, A. *Macromol. Rapid Commun.* **2005**, *26*, 82.

8. Lönnberg, H.; Zhou, Q.; Brumer, H., III; Teeri, T.; Malmström, E.; Hult, A. *Biomacromolecules* **2006**, *7*, 2178.

9. Carlmark, A.; Malmström, E. E. *J. Am. Chem. Soc.* **2002**, *124*, 900.

10. Kang, H.; Gao, X.; Ruigang Liu, R.; Huang, Y. In Functional Materials from Renewable Sources; Liebner, F.; Rosenau, T., Eds.; ACS publications, Washington, **2012**; Vol. *1107*, Chapter 6, p 109.

11. Castelvetro, V.; Geppi, M.; Giaiacopi, S.; Mollica, G. *Biomacromolecules* **2007**, *8*, 498.

12. Roy, D.; Guthrie, J. T.; Perrier, S. *Macromolecules* **2005**, *38*, 10363.

13. Krouit, M.; Bras, J.; Belgacem, M. N. *Eur. Polym. J.* **2008**, *44*, 4074.

14. Hadano, S.; Onimura, K.; Tsutsumi, H.; Yamsaki, H.; Oishi, T. *J. Appl. Polym. Sci.* **2003**, *90*, 2059.

15. Hadano, S.; Okada, N.; Onimura, K.; Yamsaki, H.; Tsutsumi, H.; Oishi, T. *Kobunshi Ronbunshu* **2003**, *60*, 454.

16. Littunen, K.; Hippi, U.; Johansson, L.-S.; Österberg, M.; Tammelin, T.; Laine, J.; Seppälä, J. *Carbohydr. Polym.* **2011**, *84*, 1039.

17. Moon, S. I.; Taniguchi, I.; Miyamoto, M.; Kimura, Y.; Lee, C. W. *High Perform. Polym.* **2001**, *13*, 189.

18. Lei, Z. Q.; Bai, Y. B.; Wang, S. F. *Chin. Sci. Bull.* **2005**, *50*, 2390.

19. Huda, M. S.; Drzal, L. T.; Mohanty, A. K.; Misra, M. *Compos. Sci. Technol.* **2008**, *68*, 424.

20. Mondal, M. I. H.; Khan, G.M.A. *Cell. Chem. Technol.* **2008**, *42*, 9.

21. Ajioka, M.; Enomoto, T.; Suzuki, K.; Yamaguchi, A. *Bull. Chem. Soc. Jpn.* **1995**, *68*, 2125.

22. Kricheldorf, H. R.; Damrau, D. O. *Macromol. Chem. Phys.* **1997**, *198*, 1753.

23. Yoo, D. K.; Kim, D.; Lee, D. S. *Macromol. Res.* **2006**, *14*, 510.

24. Yoo, D. K.; Kim, D.; Lee, D. S. *Macromol. Res.* **2005**, *13*, 68.

25. Zhang, C.; Price, L. M.; Daly, W. H. *Biomacromolecules* **2006**, *7*, 139.

26. George, J.; Sreekala, M. S.; Thomas, S. *Polym. Eng. Sci.* **2001**, *41*, 1471.

27. Yan, C.; Zhang, J.; Lv, Y.; Yu, J.; Wu, J.; Zhang, J.; He, J. *Biomacromolecules* **2009**, *10*, 2013.

28. Zhao, Q.; Wang, S.; Cheng, X.; Yam, R. C. M.; Kong, D.; Li, R. K. Y. *Biomacromolecules* **2010**, *11*, 1364.

29. Teramoto, Y.; Nishio, Y. *Polymer* **2003**, *44*, 2701.